Model of two-dimensional electron gas formation at ferroelectric interfaces

P. Aguado-Puente,[1,2,*] N. C. Bristowe,[3,4] B. Yin,[5,2] R. Shirasawa,[6,†] Philippe Ghosez,[3]
P. B. Littlewood,[7,8] and Emilio Artacho[1,2,9,10]

[1]*Donostia International Physics Center, Paseo Manuel de Lardizabal 4, 20018 San Sebastián, Spain*
[2]*CIC Nanogune, Tolosa Hiribidea 76, 20018 San Sebastián, Spain*
[3]*Theoretical Materials Physics, University of Liège, B-4000 Sart-Tilman, Belgium*
[4]*Department of Materials, Imperial College London, London SW7 2AZ, United Kingdom*
[5]*Department of Engineering Mechanics, Zhejiang University, Hangzhou 310027, China*
[6]*Department of Earth Sciences, University of Cambridge, Downing Street, Cambridge CB2 3EQ, United Kingdom*
[7]*Physical Sciences and Engineering, Argonne National Laboratory, Argonne, Illinois 60439, USA*
[8]*University of Chicago, James Frank Institute, Chicago, Illinois 60637, USA*
[9]*Theory of Condensed Matter, Cavendish Laboratory, University of Cambridge, J. J. Thomson Ave, Cambridge CB3 0HE, United Kingdom*
[10]*Basque Foundation for Science Ikerbasque, 48013 Bilbao, Spain*

The formation of a two-dimensional electron gas at oxide interfaces as a consequence of polar discontinuities has generated an enormous amount of activity due to the variety of interesting effects it gives rise to. Here, we study under what circumstances similar processes can also take place underneath ferroelectric thin films. We use a simple Landau model to demonstrate that in the absence of extrinsic screening mechanisms, a monodomain phase can be stabilized in ferroelectric films by means of an electronic reconstruction. Unlike in the $LaAlO_3/SrTiO_3$ heterostructure, the emergence with thickness of the free charge at the interface is discontinuous. This prediction is confirmed by performing first-principles simulations of free-standing slabs of $PbTiO_3$. The model is also used to predict the response of the system to an applied electric field, demonstrating that the two-dimensional electron gas can be switched on and off discontinuously and in a nonvolatile fashion. Furthermore, the reversal of the polarization can be used to switch between a two-dimensional electron gas and a two-dimensional hole gas, which should, in principle, have very different transport properties. We discuss the possible formation of polarization domains and how such configuration competes with the spontaneous accumulation of free charge at the interfaces.

I. INTRODUCTION

After the discovery of the formation of a two-dimensional electron gas (2DEG) at some oxide interfaces [1,2] it was immediately realized that this system possessed a number of potential applications. The great efforts devoted to the investigation of this unexpected phenomenon have indeed yielded a fantastic variety of functionalities that can be tailored in these systems such as superconductivity [3] or enhanced capacitance [4]. Furthermore, the occurrence of a 2DEG in a perovskite system opens possibilities for coupling such 2DEG to other interesting properties commonly found in different perovskites, from high-T_c superconductivity to multiferroicity.

The driving force for the formation of the 2DEG at oxide interfaces, such as the $LaAlO_3/SrTiO_3$ heterostructure, is the polar discontinuity at the boundary between two materials with different formal polarizations [5]. This polarization mismatch has a huge electrostatic cost and can favor the formation of free charge that accumulates at the interface in order to screen the discontinuity, the process sometimes referred to as the "polar catastrophe" [6]. One interesting aspect of this phenomenon is that the magnitude of the polar discontinuity can be tuned in a number of different ways:

using different interface orientations [7], alloying the polar material to effectively change its polarization [8], or playing with the electrostatic boundary conditions of the system [9]. One possible way to manipulate the electrostatic boundary conditions is through the coupling with ferroelectricity. This strategy has been considered in the past [10–14] since the spontaneous polarization of the ferroelectric material could be used to tune the polar mismatch at the interface. Indeed, the manipulation of the 2DEG in $LaAlO_3/SrTiO_3$ using ferroelectricity has already been achieved experimentally in different ways. In Ref. [11], epitaxial strain was used to induce a ferroelectric phase transition in $SrTiO_3$, whose spontaneous polarization was observed to partially screen the polar discontinuity, thus reducing the carrier concentration and increasing the critical thickness of $LaAlO_3$ for the formation of the 2DEG. Alternatively, in Ref. [12], Tra and coauthors used a ferroelectric overlayer to top-gate the $LaAlO_3/SrTiO_3$ heterostructure, being able to induce a metal-insulator transition at the interface in a nonvolatile way by switching the polarization of the ferroelectric. A more radical approach is directly to substitute the polar $LaAlO_3$ by a ferroelectric material and use the spontaneous polarization of the ferroelectric as the source for the polar discontinuity. This possibility has already been explored from first principles [13–15]. In Refs. [13,14] it was shown that the 2DEG could be manipulated with the ferroelectric polarization in symmetric $KNbO_3/ATiO_3$ ($A =$ Sr, Ba, Pb) heterostructures. However, the nonstoichiometry of the simulated geometry implied that the interfaces studied in

─────────
*p.aguado@nanogune.eu
†Current address: Sony Corporation, Atsugi-shi, Kanagawa, 243-0021, Japan.

those works were metallic *by construction*. In fact, it was later demonstrated [16] that since centrosymmetric $KNbO_3$ is polar with a formal polarization of half a quantum of polarization (modulo a quantum of polarization), just like $LaAlO_3$, when a [001] interface between this material and a nonpolar one is grown the *ferroelectric* polarization of $KNbO_3$ tends to compensate the polarity of the interface. As a result, the polarization of the $KNbO_3$ layer is pinned and its formal value in the ferroelectric ground state is approximately zero (up to a quantum of polarization) rendering any screening mechanism unnecessary.

Instead, a ferroelectric with a nonpolar centrosymmetric high-temperature phase should be used. In that case, the polarization in the ferroelectric phase is not intrinsically compensated. For a free-standing slab or a thin film of such material on top of an insulating, nonpolar substrate (such as the common $SrTiO_3$), the switchable polarization of the ferroelectric could be used to manipulate the electrostatic boundary conditions at the interface and possibly induce the formation of a 2DEG. This, of course, would only be possible if such configuration, a monodomain ferroelectric phase screened by a 2DEG, is stable, because, unlike $LaAlO_3$, for a ferroelectric thin film the system has alternative routes available to minimize or avoid the polarization mismatch. For one, in the absence of a screening mechanism other than the accumulation of free charge at the interface, depolarization effects might render the paraelectric configuration as the only stable homogeneous phase of the system. But, most notably, the system can break into polarization domains. Strikingly, reports of monodomain phases in ferroelectric thin films on insulating substrates are not rare in the experimental literature [17–23], even though a simple electrostatic analysis reveals that such configuration can only be stable if free charge accumulates at the interfaces. In this geometry, interface or surface atomic reconstructions, or simple adsorption of ionic species to the surface do not provide the necessary screening [24]. A transfer of charge from the surface to the interface or vice versa is needed, which, as in the case of $LaAlO_3/SrTiO_3$, might come from different sources, such as an electronic reconstruction or redox processes. In fact, a very recent first-principles study has shown that electronic reconstruction can stabilize a polarization in a $BaTiO_3$ thin film on top of $SrTiO_3$ [15]. In that work, simulations performed for a specific thickness of the ferroelectric film showed that, even if the ground state of the system was the paraelectric phase, a configuration with a finite polarization pointing towards the substrate and a 2DEG at the interface was metastable. Neither the polarization reversal nor a metal-insulator transition with thickness or electric field could be demonstrated, but the work of Ref. [15] together with all the previous arguments suggest that the formation and manipulation of a 2DEG at ferroelectric interfaces might indeed be possible.

The complex phenomenology that is expected for these systems cannot be explored exclusively within a first-principles approach. The relative stability of the polar configuration with respect to competing phases, the evolution of such competition with the thickness, or the response of the system to an external electric field (which is the main interest of having a 2DEG in ferroelectric films) are issues of prime importance for which a systematic first-principles analysis is today unfeasible. In

this work, we use a phenomenological model, supported by first-principles calculations, to confirm that ferroelectricity can be used to induce the formation of two-dimensional electron and hole gases at the interface with nonpolar substrates. We discuss the conditions for the stability of such configuration, its coupling with external electric fields [which gives rise to a discontinuous switching (on and off) of the gas] and its competition with alternative screening mechanisms such as the formation of polydomain phases. The paper is organized as follows: In Sec. II we present the model and use it to predict the range of stability of a 2DEG in a prototypical system, in Sec. III we analyze the interaction with an external electric field, and in Sec. IV we discuss the implications of the results, in particular how they are affected by the competition with polydomain phases and what is the expected phenomenology in the case of the recently proposed hyperferroelectric materials [25].

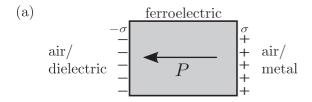## II. FORMATION OF A 2DEG AT FERROELECTRIC INTERFACES

A. A simple model

Phenomenological models have been successfully used to rationalize the formation of a 2DEG at polar interfaces between paraelectric materials [24,26]. These models allow to assess the viability of different processes able to screen the polar discontinuity by injecting free charge into the interfaces/surfaces. Here, we use the same formalism to explore the formation of a 2DEG at ferroelectric thin films. We first consider the possible transition from paraelectric to ferroelectric with a 2DEG, neglecting the competition with the formation of domains (discussed in Sec. IV A).
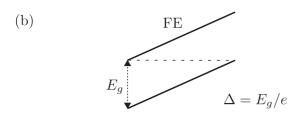
We start assuming that no extrinsic mechanisms contribute to the screening, thus the electronic reconstruction (for which electrons from one surface/interface are transferred to the opposite one to screen the polarization of the film) is the only possible source of free charge [24]. Throughout this paper, for the sake of conciseness, we only speak about 2DEG, but it should be noted that under the assumption of electronic reconstruction, the formation of a 2DEG implies the appearance of a corresponding two-dimensional hole gas (2DHG) at the opposite interface or surface. Later on, we discuss how this model can also be used to describe the basic behavior of the system when the free carriers are provided by surface redox processes (like formation of charged defects or adsorption of chemical species).
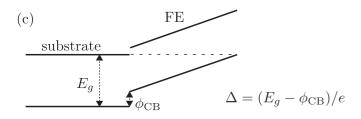
If the 2DEG forms as a result of electronic reconstruction, the free energy *per unit volume* of a ferroelectric thin film of thickness d reads as

$$G = U + \frac{\sigma \Delta}{d} + \frac{\sigma^2}{2gd} + \frac{1}{2\varepsilon_0}(\sigma - P)^2 . \quad (1)$$

In this expression, U is the free energy of the bulk ferroelectric at zero field, that depends on the polarization P. The next two terms on the right-hand side of Eq. (1) account for the energy cost of promoting electrons from the top of the valence band to the bottom of the conduction band. The second term of the equation corresponds to the cost of the charge transfer across the gap, where σ is the surface density of free charge, and Δ is the "relevant band gap" of the system in units of a voltage. Neglecting surface effects, Δ is equal to the
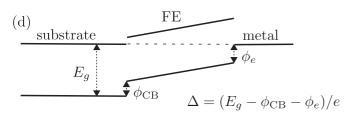
FIG. 1. (a) Schematic diagram of the geometry of the system. The sign criterion in all the equations throughout the paper assumes absolute values of both the polarization and the free-charge density, and their relative orientation is the one given in this figure. (b)–(d) Schematic band alignment for a ferroelectric thin film in various configurations. The corresponding value of the relevant gap Δ; the band offset at the interface ϕ_{CB}; and the Shottky barrier for electron in the presence of an electrode ϕ_e are indicated in each case.

of charge squared per units of area and energy, with g_e and g_h being the density of states (DOS) for electrons and holes, respectively (we take the densities of states as constants, as in a free-electron gas in 2D). The last term in Eq. (1) corresponds to the electrostatic energy of the remnant depolarizing field, and constitutes the driving force for the formation of the 2DEG.

There are several subtleties regarding Eq. (1) that should be noted. First, our Landau-type model is restricted to an out-of-plane polarization; it does not include the possibility of in-plane polarization nor any explicit strain dependence. Some simple mechanical boundary conditions, such as epitaxial strain, can be implicitly accounted for by a renormalization of the coefficients in the expansion of U [27]. The generalization needed to explicitly include these additional degrees of freedom is nevertheless trivial: U would depend on the three components of the polarization and on the strain, the out-of-plane component of P being the only relevant one in the depolarization term. Such a model would allow for a rotation of the polarization in plane, which in some cases might be a competing mechanism to avoid the electrostatic cost associated to a discontinuity of the out-of-plane polarization. Such possibility is, however, not discussed here because the in-plane epitaxial compressive strain imposed by the substrate hinders the stability of an in-plane polarization in the prototypical systems of interest (such as epitaxial $PbTiO_3$ or $BaTiO_3$ on $SrTiO_3$). Second, in Eq. (1) we assume that the distance between electron and hole layers is large enough that exchange interactions, as well as excitonic binding, can be disregarded. Finally, throughout this paper, both σ and P are the magnitudes of the physical quantities and the signs of the different terms in all the equations are valid for the geometry and relative orientation of σ and P depicted schematically in Fig. 1(a). For an arbitrary sign of the free charge with respect to the polarization, one should take into account that the term corresponding to the band-gap energy should read as $|\sigma|\Delta$. Furthermore, since the orientation of the polarization has a strong influence on the band alignment of an interface, the relevant gap may, in general, have a different value for opposite orientations of the polarization. This difference, together with the choice of a suitable thickness, might be exploited to switch on and off the 2DEG, as will be discussed in the following.

For prototypical ferroelectric materials *at zero electric field*, the relevant free energy can be expressed as a Landau expansion in terms of a single-order parameter responsible for the ferroelectric phase transition η, which for these materials consists of a soft mode associated to a collective shift of the oxygen cage with respect to the cations. Alternatively, one can use the polarization associated with this mode $P_\eta = \frac{1}{\Omega}Z_\eta^*\eta$, where Ω is the unit-cell volume of the ferroelectric and Z_η^* is the Born effective charge associated with the mode η. The Landau expansion of the free energy per unit volume in terms of this polarization is expressed as

$$U_0 = \frac{1}{2}a(T - T_C)P_\eta^2 + \frac{1}{4}bP_\eta^4 + \mathcal{O}(P_\eta^6), \quad (2)$$

where T_C is the Curie temperature of the material. For materials with a second-order phase transition with the temperature, the coefficients of P_η^4 and larger-order terms are positive and the energy expansion of Eq. (2) may be truncated at the quartic term. This allows most of the analysis that follows to be done in terms of analytical expressions and provides a direct

band gap of the ferroelectric in the case of a free-standing slab [see Fig. 1(b)], but in general its value depends on the configuration of the heterostructure. Figure 1 illustrates different cases, where Δ is calculated from the band gap of the constituent materials, the band alignment across interfaces, and the Fermi level of a top electrode (if present). If band bending or any other modification of the electronic structure occurs at the interfaces, it should also be taken into account. Throughout this paper, for the numerical estimations we will consider the simplest approximation and use the band gap of the bulk ferroelectric for Δ. The third term in Eq. (1) takes into account the energy associated to the filling of the bands (the conduction band with electrons and the valence band with holes). This energy cost is associated with a finite density of states. The "reduced density of states" [24] used in Eq. (1) is calculated as $g = (g_e g_h)/(g_e + g_h)$ and is expressed in units

relationship between the constants in the Landau expansion and common physical properties such as the spontaneous polarization and susceptibility. A more general discussion should take into account higher-order terms and, as in the case of improper ferroelectrics, the coupling of polar modes with nonpolar distortions. However, here we restrict ourselves to materials which can be described by the expression in Eq. (2) since this includes some prototypical systems such as BaTiO$_3$ and PbTiO$_3$ under compressive epitaxial strain [27] (again, this is the case if either of these materials is grown on a SrTiO$_3$ substrate). In fact, since the phenomenology described in this work is a consequence of the "double-well" shape of the free energy as a function of the polarization of ferroelectrics, the behavior derived from the model should also be qualitatively valid for ferroelectrics with a first-order phase transition provided that $T \ll T_C$.

At a given temperature below the phase transition (and leaving temperature aside for the time being), we rewrite Eq. (2) as

$$U_0 = \frac{1}{2\varepsilon_0\chi_\eta}\left(\frac{1}{4}\frac{P_\eta^4}{P_S^2} - \frac{1}{2}P_\eta^2\right), \tag{3}$$

where $P_S = [(a/b)(T_C - T)]^{1/2}$ is the spontaneous polarization in the absence of a depolarizing field, and $\varepsilon_0\chi_\eta = [2a(T_C - T)]^{-1}$ is the contribution of η to the polarizability around P_S. χ_η would correspond to the curvature around the minimum of the double-well energy curve $U_0(P_\eta)$, typically obtained from first principles performing a series of frozen phonon calculations at zero field. The expression in Eq. (3), however, is only valid at zero field since it does not include the extra polarization of the electrons and other phonons in arbitrary electrostatic boundary conditions. In general, the Landau expansion of the energy would be

$$U = \frac{1}{2\varepsilon_0\chi_\eta}\left(\frac{1}{4}\frac{P_\eta^4}{P_S^2} - \frac{1}{2}P_\eta^2\right) + \frac{1}{2\varepsilon_0\chi_\infty}P_e^2, \tag{4}$$

where the total polarization of the material is

$$P = P_\eta + \varepsilon_0\chi_\infty\mathcal{E} = P\eta + P_e. \tag{5}$$

Note that P_η already includes a contribution from the electronic cloud contained in Z_η^* since this is a dynamical charge that takes into account the deformation of the electronic charge density with the amplitude of the polar distortion at zero field. Accordingly, P_e and χ_∞ are the extra polarization and susceptibility due to the presence of a finite electric field. P_e and χ_∞ account mainly for the polarizability of the electronic cloud, thus we will refer to them as *electronic* polarization and susceptibility throughout the paper; however, strictly speaking, these two terms also include the contribution of hard modes of the lattice [28,29]. Using the electrostatic boundary conditions of our problem we can express P_e in terms of the total polarization P as

$$P_e = \varepsilon_0\chi_\infty\mathcal{E} = \varepsilon_0\chi_\infty\frac{\sigma - P}{\varepsilon_0} = \chi_\infty(\sigma - P), \tag{6}$$

which, in turn, can be written as a function of the zero-field polarization as

$$P = \frac{P_\eta + \chi_\infty\sigma}{\varepsilon_\infty}, \tag{7}$$

where $\varepsilon_\infty = \chi_\infty + 1$ is the electronic (or background) contribution to the relative permittivity of the ferroelectric. Using Eqs. (5)–(7), Eq. (1) transforms into

$$G = \frac{1}{2\varepsilon_0\chi_\eta}\left(\frac{1}{4}\frac{P_\eta^4}{P_S^2} - \frac{1}{2}P_\eta^2\right)$$
$$+ \frac{1}{2\varepsilon_0\varepsilon_\infty}(\sigma - P_\eta)^2 + \frac{\Delta\sigma}{d} + \frac{\sigma^2}{2gd}. \tag{8}$$

Note that the second term in Eq. (8) looks very similar to the last term in Eq. (1) and consequently it could be misunderstood as the energy due to the depolarizing field, but in fact it contains that contribution as well as the one due to the electronic polarization P_e.

Equation (8) can be used to find the equilibrium polarization and surface/interface free charge in a ferroelectric thin film. We will neglect for the moment the influence of the DOS assuming that g is relatively large. Since the DOS term is inversely proportional to g, it decays rapidly for relatively large, but realistic, values of the DOS. Therefore, the approximation $g \to \infty$ can be made without significantly affecting the qualitative behavior of the system and simplifying the analysis that follows. Under this approximation, the two equilibrium conditions $\partial G/\partial P_\eta = \partial G/\partial \sigma = 0$ yield the system of equations

$$\frac{P_\eta^3}{P_S^2} - P_\eta - \frac{2\chi_\eta}{\varepsilon_\infty}(\sigma - P_\eta) = 0, \tag{9}$$
$$\frac{\Delta}{d} + \frac{1}{\varepsilon_0\varepsilon_\infty}(\sigma - P_\eta) = 0 \tag{10}$$

under the constraint of $\sigma \geqslant 0$. In the limit of large film thickness, the solutions of these two equations are $\sigma = P_\eta$ and $P_\eta = \{-P_S, 0, P_S\}$; and, using Eq. (7), $P = P_\eta$. This just means that in thick ferroelectric films, the bulk tendency dominates, polarizing accordingly, and the free charge at the surfaces just follows, precisely canceling the depolarizing field (as in shorted boundary conditions). As d decreases from ∞, P_η diminishes, but σ diminishes faster, leaving part of the polarization uncompensated (the energy cost of the depolarizing field does not completely overwhelm the energy cost of transferring charge from the valence to the conduction band Δ).

In order to study the thickness dependence of the equilibrium polarization and free-charge density, Eqs. (9) and (10) can be combined to obtain the condition

$$\frac{P_\eta^3}{P_S^3} - \frac{P_\eta}{P_S} + \frac{l}{d} = 0, \tag{11}$$

where

$$l = 2\chi_\eta\frac{\varepsilon_0\Delta}{P_S} \tag{12}$$

is a characteristic length scale for a given set of parameters. In the plot of P or σ versus d, the bulk spontaneous polarization P_S defines the scale for P and σ, and the length l defines the scale for film thickness d.

The evolution of both P and σ is shown in Fig. 2 as a function of d. For this plot we used the parameters for PbTiO$_3$ obtained from first principles [30] except for Δ, for which
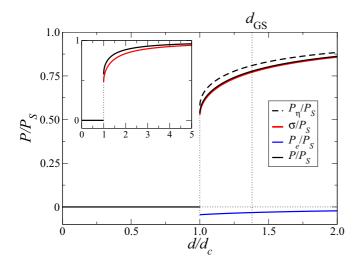
FIG. 2. (Color online) Total polarization (black solid line), zero-field contribution (dashed line), electronic contribution (solid blue line), and surface free charge (solid red line) versus ferroelectric film thickness (d). P_S is the spontaneous polarization of the bulk ferroelectric material, d_c is the critical thickness for the onset of ferroelectric metastability, and d_{GS} is the thickness at which the ferroelectric configuration becomes the ground state of the system. Inset: same plot with $\chi_\eta = 2$ and $\varepsilon_\infty = 1$ to highlight the convergence of σ towards P (in this situation $P = P_\eta$).

we used the experimental band gap, i.e., $e\Delta = 3.6$ eV. The thick film limit (large d) displays what was described before, namely, (i) P tends to the bulk value P_S, and (ii) the free-charge density σ tends to screen the polarization. The polarization then diminishes for thinner films until a critical thickness

$$d_c = l\frac{3\sqrt{3}}{2}, \tag{13}$$

where a discontinuous jump in all magnitudes occur, and below which $P = \sigma = 0$. The value of the polarization at the critical thickness is

$$P_\eta^c = \frac{P_S}{\sqrt{3}}, \tag{14}$$

independent of other parameters. The implications of Eqs. (13) and (14) are quite remarkable, in the sense that these expressions suggest that this is a rather general behavior for ferroelectric materials [at least for those which respond to the energy expression of Eq. (2)], and that the main fingerprints of the phenomenon are determined by the bulk properties of the material.

It is interesting to note that the equilibrium screening of P by interfacial free charge is quite effective for any thickness. The inset in Fig. 2 assumes a value of $\chi_\eta = 2$ for the plots of σ and P versus d, which was chosen for illustrative purposes, but represents a very small value for any real material. Indeed, a more realistic value ($\chi_\eta = 27$ for PbTiO$_3$) pushes the σ curve right onto the P curve, as shown in Fig. 2.

Figure 3 shows how the solution in Fig. 2 arises. The energy functional of Eq. (8) has two possible sets of solutions. For $\sigma = 0$, the energy of the system as a function of the polarization is a parabola, as in a dielectric material, and the equilibrium solution is $P_\eta = P = 0$. Instead, the energy
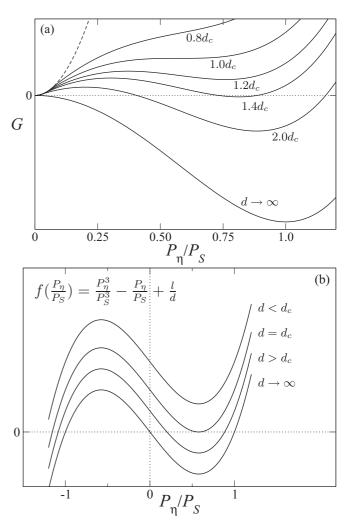

FIG. 3. (a) Energy per unit volume as a function of polarization for various thicknesses. The numbers next to the curves indicate the values of the thickness in each case. Dashed line corresponds to a solution with $\sigma = 0$ while solid lines are the curves with $\sigma \neq 0$. Curves with $\sigma \neq 0$ possess an equilibrium configuration only for $d \geqslant d_c$. (b) Graphical solution of the equilibrium condition given by Eq. (11).

curve for $\sigma \neq 0$ [solid lines in Fig. 3(a)] has extrema given by Eq. (11). The function $f(p) = p^3 - p$, corresponding to the limit of $d \to \infty$ of Eq. (11) and plotted in Fig. 3(b), has roots at -1, 0, and 1. As d is reduced, the cubic curve shifts upward, then the upper root (corresponding to the polarization of the equilibrium ferroelectric configuration) diminishes while the middle one [corresponding to the energy bump in the $G(P_\eta)$ curves of Fig. 3(a)] becomes positive. The consequence of this is that an energy barrier, which amplitude decays asymptotically as $d \to \infty$, separates the paraelectric and ferroelectric configurations for every $d > d_c$ and the system possesses three stable states: zero polarization (insulating state) and the two opposite polarization orientations (2D metallic state). Furthermore, as can be seen in Fig. 3(a), there is a range of thicknesses $d_c < d < d_{GS} \sim 1.4 d_c$ for which the ground state of the system is the paraelectric configuration, and the ferroelectric one screened by the electronic reconstruction is a local energy minimum. At the critical thickness d_c the

minimum of the cubic curve touches the axes, meaning that at lower values of d the upper root becomes imaginary and ferroelectric configuration ceases to be stable.

The physical interpretation of the phenomenology described above is clear: the appearance of spontaneous polarization in the film requires the screening of the depolarizing field. This is accomplished by the accumulation of free charge that results in the formation of the corresponding 2DEG at the interface. Being the screening processes a surface effect and the tendency to polarization a bulk effect, the latter dominates for thick enough films, while the former dominates in thin films.

Interestingly, the transition from paraelectric to ferroelectric or, analogously, from an insulating to a conductive interface, is discontinuous. This contrasts with the case of the LaAlO₃/SrTiO₃ interface for which an effective model like this predicts a continuous transition with a gradual decrease of the interface charge as the LaAlO₃ thickness is reduced [24]. This of course cannot be observed experimentally since the thickness of LaAlO₃ can only be varied in units of the out-of-plane lattice constant c. The continuous metal-insulator transition in SrTiO₃/LaAlO₃ can be shown using an external field to deplete charge from the 2DEG [9,31,32]. For the ferroelectricity-induced 2DEG we will confirm the discontinuous transition under the application of an external electric field in Sec. III.

1. Estimates

In addition to insights into the character of the transition, the model, still within the $g \to \infty$ approximation, allows estimations of the relevant magnitudes. As stated above, the jump in polarization P_η^c is $P_S/\sqrt{3} \sim 0.6 P_S$ and is thus quite universally defined, just dependent on the equilibrium polarization of the bulk ferroelectric material.

For the critical film thickness d_c, we can get estimates by comparing the results obtained for the LaAlO₃/SrTiO₃ interface [24] and for the ferroelectric film [Eqs. (12) and (13)]

$$d_c^{\text{LAO}} = \frac{(1+\chi^{\text{LAO}})}{P_0^{\text{LAO}}}\varepsilon_0 \Delta^{\text{STO}} \; ; \; d_c^{\text{F}} = \frac{3\sqrt{3}\chi_\eta^{\text{F}}}{P_S^{\text{F}}}\varepsilon_0 \Delta^{\text{F}}, \quad (15)$$

where F stands for ferroelectric, and P_0^{LAO} refers to half a quantum of polarization. Assuming similar values of the band gap, and considering now that the critical thickness for LaAlO₃ on SrTiO₃ is around four perovskite layers, and that $3\sqrt{3}\sim 5$,

$$d_c^{\text{F}} \sim 20\big(\chi_\eta^{\text{F}}/\chi^{\text{LAO}}\big) \text{ layers}, \quad (16)$$

which can grow quite thick depending on how close the temperature is to the bulk ferroelectric T_c.

2. Effect of a finite density of states

For simplicity, we have assumed so far a large value of the reduced DOS g. This approximation allowed us to neglect the energy cost of the filling of the valence and conduction bands, simplifying the analysis. The effect of a finite DOS is to penalize the accumulation of free charge and consequently it is expected to shift to larger thicknesses the metal-insulator transition. To analyze how important the
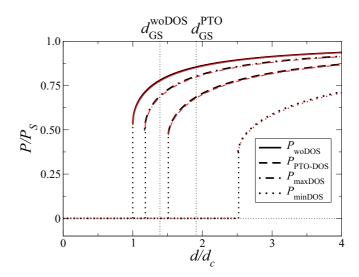

FIG. 4. (Color online) Total polarization (black) and free charge (red) versus thickness calculated using different values for the DOS g. The different approximations for g are $g \to \infty$ (solid lines), the value corresponding to PbTiO₃ obtained from its bulk band structure [30] (dashed lines), and the two extrema of an estimated range of values for this family of materials (top limit in dashed-dotted and bottom limit in dotted lines, respectively).

influence of a finite DOS is, we plot in Fig. 4 the curves of polarization as a function of thickness for various values for the DOS g. For PbTiO₃, we estimated the corresponding two-dimensional DOS for electrons and holes from the bulk band structure obtained from first principles. In addition to the usual considerations to calculate a DOS, in these systems one should also take into account the fact that the interface lifts some degeneracies. We use the results of Refs. [33,34], which showed that after the electronic reconstruction the bottom of the conduction band in perovskite titanates has a d_{xy} character, to estimate a DOS for electrons of $g_e/e^2 = 1.2 \times 10^{37}$ m⁻²J⁻¹ (1.9×10^{14} cm⁻²eV⁻¹ in more conventional units). We performed a similar analysis for the valence band [35] to obtain the corresponding DOS for holes, which amounts to $g_h/e^2 = 2.5 \times 10^{37}$ m⁻²J⁻¹ (4.0×10^{14} cm⁻²eV⁻¹). Using the estimated DOS for PbTiO₃ we observe that there is a significant increase of the transition thickness to about $\sim 1.5 d_c$, where d_c is given by Eq. (13) in the limit of $g \to \infty$. The values of d_c and d_{GS} predicted by the model for PbTiO₃, both in the limit of $g \to \infty$ and for a finite and realistic DOS, can be found in Table I. According to the values in Table I, the thickness necessary to produce a 2DEG in a ferroelectric thin film is large compared with the case of the LaAlO₃/SrTiO₃ interface. For

TABLE I. Critical thickness for the stability of a 2DEG induced by ferroelectricity d_c and for the polar phase to become the ground state with respect to a paraelectric configuration d_{GS}. The thicknesses are calculated both in the limit of infinite DOS and using a realistic value for bulk PbTiO₃ [30].

	d_c (nm)	d_{GS} (nm)
Without DOS	5.5	7.7
With DOS	8.3	10.5

ferroelectrics grown under a high epitaxial strain, mechanisms for strain relaxation might start playing a role in this range of thicknesses, something that would affect the parameters in the model. This is not the case for $PbTiO_3$ on $SrTiO_3$, the system chosen for the numerical estimations throughout this paper, for which epitaxy over thicknesses of several hundreds of unit cells can be achieved [36]. Furthermore, the critical thicknesses in Table I can be be potentially reduced by an appropriate choice of materials, and the model presented here provides a simple tool for the screening of optimal systems.

Taking into account how large the effect of the DOS can be, it is worthwhile to explore a range of sensible values since different substrates, terminations, or sources of free charge (see next section) could give rise to very different values of g. If the source of free charge is, as assumed so far, an electronic reconstruction and the materials involved in the formation of the interface are oxide perovskites, from the estimated values g_e and g_h for $PbTiO_3$ we can consider that a given material of this family probably displays a DOS in the range between 5×10^{36} to $5 \times 10^{37} \, \mathrm{m^{-2} J^{-1}}$ (8.0×10^{13} to $8.0 \times 10^{14} \, \mathrm{cm^{-2} eV^{-1}}$). These two values are used to calculate the two extra curves in Fig. 4. Inspecting Fig. 4, one can see that in fact materials with a large, but still reasonable, DOS might show a dependence of the polarization with respect to the thickness very close to the ideal situation. In materials with a low DOS, on the other hand, the transition may take place at thicknesses as large as $2.5d_c$–$3d_c$.

The strong influence of a finite DOS on the critical thickness for the onset of a 2DEG in ferroelectric films is especially noteworthy because such dependence does not appear in the case of the $LaAlO_3/SrTiO_3$ interface. In fact, it was demonstrated in Ref. [24] that a model for polar interfaces between dielectric materials analogous to the one presented here yields a critical thickness for the formation of the 2DEG that is independent of the DOS [see Eq. (18) in the aforementioned paper].

3. Other sources of free charge

Although the electronic reconstruction was the first mechanism for the formation of the 2DEG in polar interface to be proposed [6], alternative processes can also yield free carriers to screen the polarization discontinuity [24]. Most notably, surface electrochemical processes such as adsorption of chemical species or formation of defects induced by the internal electric field in the film are believed to play a major role in the screening at ferroelectric thin films [37–41] and polar interfaces [26,42–44]. To account for this kind of mechanism, Eq. (1) may be rewritten as

$$G = U + \frac{Cn}{d} + \frac{\alpha n^2}{2d} + \frac{1}{2\varepsilon_0}(nQ - P_\eta)^2 \,, \qquad (17)$$

where C is the formation energy of an isolated redox defect in the absence of an electric field and Q is the charge provided by the defect. The defect-defect interaction is accounted for in a mean-field approximation by the term $\alpha n^2/2d$. It is easy to show that Eqs. (17) and (1) are in fact equivalent by simply making $\sigma = nQ$, $\Delta = C/Q$, and $\alpha = Q^2/g$. Indeed, the analysis presented above for electronic reconstruction is parallel to any other planar charge screening mechanism

associated with an energy cost per surface/interface charge. This allows us to treat any equivalent screening mechanism with the same equations, by considering the surface density of free charge σ, and taking into account the "effective" gap and DOS relevant for each process. An analysis of the behavior under the simultaneous presence of more than one mechanism can also be done, as in Ref. [24] for $LaAlO_3/SrTiO_3$.

4. Assuming given σ or P

The analysis in the previous subsections assumes equilibrium, and thus neglects any kinetic effects, which can be very important, e.g., in the formation of defects or the Zener tunneling of the carriers across the film. In some occasions, such kinetic effects may dominate. We can easily consider the situation in which a certain concentration of redox defects n has been generated on the surface, e.g., at growth, which are then frozen in. Such scenario corresponds to a ferroelectric layer in open boundary conditions with fixed electric displacement D, where $D = \sigma = nQ$. In this situation, σ is not a variable but the parameter determining the electrostatic boundary conditions of the system. The relevant free energy is now simply [45]

$$G = U + \frac{1}{2\varepsilon_0}(\sigma - P)^2. \qquad (18)$$

Using again the transformations for P given by Eqs. (6) and (7) we get

$$G = \frac{1}{2\varepsilon_0 \chi_\eta}\left(\frac{1}{4}\frac{P_\eta^4}{P_S^2} - \frac{1}{2}P_\eta^2\right) + \frac{1}{2\varepsilon_0 \varepsilon_\infty}(\sigma - P_\eta)^2. \qquad (19)$$

We can then ask what would be the equilibrium polarization P for given values of σ. Minimizing G with respect to P gives the equation

$$\frac{P_\eta^3}{P_S^3} + \left(\frac{2\chi_\eta}{\varepsilon_\infty} - 1\right)\frac{P_\eta}{P_S} - \frac{2\chi_\eta \sigma}{\varepsilon_\infty P_S} = 0\,, \qquad (20)$$

where the last term is a constant. For any $\chi_\eta/\varepsilon_\infty > \frac{1}{2}$, this equation has a single real root, which is positive. Considering for simplicity a large value of $\chi_\eta/\varepsilon_\infty$, and for values of σ not much larger than P_S, the solution can be approximated by

$$P_\eta \sim \sigma + \frac{\varepsilon_\infty}{2\chi_\eta}\sigma\left[1 - \left(\frac{\sigma}{P_S}\right)^2\right], \qquad (21)$$

which using Eq. (7) transforms into

$$P \sim \sigma + \frac{1}{2\chi_\eta}\sigma\left[1 - \left(\frac{\sigma}{P_S}\right)^2\right]. \qquad (22)$$

That is, the polarization responds by compensating the effective polarization given by the 2DEG carriers (first term) except for a small deviation, which is positive ($P > \sigma$) for $\sigma < P_S$ and negative for $\sigma > P_S$, or, in other words, the polarization tends to screen the field generated by the fixed surface/interface charge, but with a slight tendency towards P_S. Note that under fixed D boundary conditions the free energy of the system scales with the volume (it does not have surface terms) and thus the behavior obtained is independent of film thickness. Several works [39,41] have demonstrated

that the manipulation of the surface chemistry can be used to switch the polarization of a ferroelectric. Furthermore, the first-principles simulations presented in Ref. [41] showed how the polarization of a $BaTiO_3$ film followed the charge density set by charged defects at the surface, as predicted by Eq. (22).

Similarly, one could ask what would be the equilibrium concentration of free charge if the polarization P had been frozen in by some mechanism. In such (unlikely) case, we would minimize Eq. (8) with respect to σ for fixed P_η and then use Eq. (7), obtaining

$$\sigma = P - \frac{\varepsilon_0 \Delta}{d}, \qquad (23)$$

which gives a phenomenology very similar to the cases of the $LaAlO_3$/$SrTiO_3$ interface, in which the polarization is also fixed (in that case to half a quantum) [24].

B. First-principles simulations

In order to test the validity of the model, its predictions can be compared with results obtained from first-principles simulations of ferroelectric thin films. Bearing in mind that first-principles simulations are typically performed at zero temperature, the results obtained with this method should be compared with the low-temperature limit of the model. Nevertheless, as long as the temperature is relatively far from the transition one, the phenomenology should be qualitatively the same.

The study presented in Ref. [15], showing that electronic reconstruction can stabilize a spontaneous polarization in symmetrical $BaTiO_3$/$SrTiO_3$ heterostructures, constitutes the first argument supporting the model. In addition to this, here we perform additional DFT calculations on a model system consisting of a slab of $PbTiO_3$ (PbO terminated on both sides) in vacuum. An in-plane lattice constant of 3.874 Å was chosen to mimic the strain of a $SrTiO_3$ substrate (which is not explicitly included in the calculation). Even though such geometry is not representative of typical experimental devices, and properties of the 2DEG such as its confinement or the mobility of the charge carriers would be very different from more realistic samples like those depicted in Figs. 1(c) and 1(d), we choose here this simple test case with the sole purpose of illustrating some of the basic predictions of the model. The calculations were performed within the local density approximation, using the SIESTA code [46]. Reciprocal space integrations were carried out on a Monkhorst-Pack [47,48] k-point grid equivalent to $6 \times 6 \times 6$ in a five-atom perovskite unit cell. For real-space integrations, a uniform grid with an equivalent plane-wave cutoff of 600 Ry was used. A dipole correction was introduced to avoid spurious interaction between periodic images of the slab along the out-of-plane direction. Initial coordinates were generated stacking m unit cells of "bulk-strained" $PbTiO_3$ in the ferroelectric phase. Starting from the polar configuration, we expect that during relaxation the system will remain in the metastable configuration predicted by the model for $d > d_c$. Then, all the atomic coordinates of the slabs were relaxed until the forces were smaller than 0.04 eV/Å.

In Table II, we list the equilibrium polarization and energies of the resulting structures as a function of the thickness. It was

TABLE II. Evolution of the polarization and the energy with respect to the nonpolar phase for $PbTiO_3$ slabs in vacuum. Here, we report the values of the polarization of stable structures after geometry optimizations initialized in a polar configuration, for $d \leqslant 12$ the system spontaneously goes back to the paraelectric phase during the relaxation. Energies are given per formula unit.

d (unit cells)	d (nm)	P/P_S	G_{FE}-G_{para} (meV)
10	4.0	0	
12	4.8	0	
14	5.6	0.52	43
16	6.4	0.62	32
18	7.2	0.79	25

found that for all slabs with $d \leqslant 12$ unit cells the atoms moved back to the centrosymmetric positions and the system was insulating. Instead, for $d \geqslant 14$ unit cells the slab remained polar and the surfaces were metallic. Within the range of thicknesses analyzed here, the energy of the system in the polar phase is higher than in the paraelectric one, confirming that the ferroelectric/2DEG configuration is still metastable, but the energy difference decreases rapidly with increasing thickness suggesting that d_{GS} should be around 10 nm.

We can now obtain the predicted critical thickness for this material according to the model. The four parameters χ_η, P_S, Δ, and c needed to estimate the critical thickness were independently computed from DFT calculations on "bulk-strained" $PbTiO_3$ and found to be 27, 0.78 C/m², 1.6 V, and 4.03 Å, respectively. The fact that the model parameters were obtained from first-principles calculations means that they also represent the low-temperature limit and a direct comparison with the first-principles simulations of the slab can be made. Using Eqs. (13) and (12), one gets $d_c = 2.4$ nm ∼6 unit cells, a value significantly smaller than the one estimated from the first-principles simulations. Nevertheless, if a reasonable value of the DOS is used ($g_e/e^2 = 1.2 \times 10^{37}$ and $g_h/e^2 = 2.5 \times 10^{37}$ m^{-2}J^{-1} for electrons and holes, as in Fig. 4) the critical thickness increases up to 5.1 nm ∼13 unit cells, in excellent agreement with the simulations.

III. SWITCHING THE 2DEG WITH AN EXTERNAL APPLIED FIELD

The main interest of having a 2DEG in a ferroelectric thin film is that the polar discontinuity at the interface might be manipulated in nontrivial ways with the application of an external electric field. Since the formation of a 2DEG relies on the presence of a polarization mismatch at the interface, the standard geometry for ferroelectric capacitors, with the bottom electrode deposited between the substrate and the ferroelectric film, cannot be used. Instead, in order to preserve the polarity of the interface, the electrodes for the manipulation of the 2DEG should be placed underneath the dielectric substrate and on top of the ferroelectric surface (the latter can be the tip of an atomic force microscope), adopting the field-effect transistor geometry often used to electrically tune the 2DEG at the $LaAlO_3$/$SrTiO_3$ interface [31,32,49] (see for instance Fig. 1 of Ref. [32]).

One obvious possible application for this system is the nonvolatile switching of the 2DEG at the interface. If the two interfaces or surfaces of the ferroelectric thin film are equivalent, switching the direction of the polarization would simply exchange the 2DEG and 2DHG between opposite interfaces. If, instead, the interfaces are dissimilar (if one of them is actually a surface, for instance) switching the polarization might also change the effective band gap Δ, modifying the value of the critical thickness d_c. If the thickness of the ferroelectric layer is close to d_c, switching the polarization would then induce a metal-insulator transition at the interface. This, however, requires the application of large electric fields to be able to switch the polarization of the ferroelectric layer, even larger than for the bulk material since the free charge of the 2DEG might respond to the electric field and screen it. Nevertheless, as we will see here, switching the polarization is not the only way to turn on and off the 2DEG at a ferroelectric interface.

To evaluate the effect of an external electric field in a ferroelectric thin film with a 2DEG at one of its interfaces, we extend the model introduced in previous sections, adding to Eq. (8) a new term corresponding to the interaction of the uncompensated polarization with the external field:
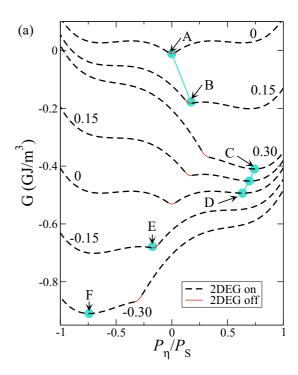
$$G = U + \frac{\sigma \Delta}{d} + \frac{\sigma^2}{2gd} + \frac{1}{2\varepsilon_0}(\sigma - P)^2 + (\sigma - P)\mathcal{E}. \quad (24)$$

In this expression, a positive value of $\mathcal{E}$ represents an electric field parallel to and with the same sign of the polarization. It should be noted that $\mathcal{E}$ is an *external* electric field and the total field experienced by the ferroelectric is $\mathcal{E}_{\text{FE}} = \mathcal{E} + (\sigma - P)/\varepsilon_0$, with the correct sign criterion. The choice of the electric field as the independent variable is in this case natural since the dependence of the polarization on $\mathcal{E}$ only involves the characteristics of the ferroelectric layer. In experiments, however, the variable that can be directly controlled is typically a gate voltage. In such case, the dependence of the polarization with the gate voltage requires also knowing details about the substrate. Nevertheless, given the specific details of a device, the relation between $\mathcal{E}$ and a gate voltage can be obtained through

$$V = \mathcal{E}\left(\frac{d_{\text{I}}}{\varepsilon_{\text{I}}} + d\right) - \frac{P - \sigma}{\varepsilon_0}d, \quad (25)$$

where d_{I} and ε_{I} are the thickness and relative permittivity of the insulating substrate. With this expression one can estimate, for instance, that for a 300-nm-thick $SrTiO_3$ substrate, with a relative permittivity of 300, the maximum electric field considered in this section ($0.4P_S/\varepsilon_0$) requires the application of approximately 30 V between the top and bottom electrodes.

The equilibrium polarization of the ferroelectric under an applied electric field $\mathcal{E}$ is found after writing Eq. (24) in terms of P_η, using again Eq. (7), and imposing the equilibrium condition $\partial G/\partial P_\eta = \partial G/\partial \sigma = 0$. To analyze the evolution of the polarization and free charge as a function of the applied electric field, it is important to recall that the energy curves plotted in Fig. 3 are actually the result of merging two curves corresponding to two different sets of solutions, one for solutions with $\sigma = 0$ and another one for solutions with $\sigma \neq 0$. In Fig. 5(a), we plot as red solid lines and black
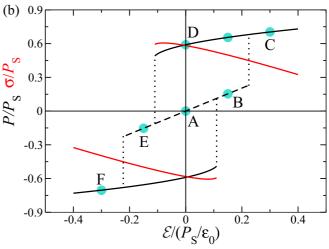

FIG. 5. (Color online) (a) Energy curves for a ferroelectric thin film as a function of the polarization for different values of the applied electric field (numerical labels next to the curves, in units of P_S/ε_0). Red solid (black dashed) sections correspond to solutions with $\sigma = 0$ ($\sigma \neq 0$). Energy curves have been shifted vertically for clarity. Light blue dots indicate equilibrium states as $\mathcal{E}$ is swept. Connected (disconnected) dots represent a continuous change (jump) in P_η. (b) Hysteresis loop for P (black line) and σ (red line) as a function of the applied electric field. For the polarization, solid lines represent the ferroelectric state with the 2DEG while the dashed lines correspond to the paraelectric phase. Both (a) and (b) are calculated for a $PbTiO_3$ thin film with a thickness of 9 nm ($d \gtrsim d_c \sim 8.3$ nm). Points labeled in the top panel correspond to those indicated in bottom panel (please find a detailed description in the text).

dashed lines the curves corresponding to $\sigma = 0$ and $\sigma \neq 0$, respectively, for a 10-nm-thick $PbTiO_3$ film and various values of the applied electric field. Since Eq. (24) is only valid for $\sigma > 0$, the sections of the curves corresponding to an electric

field antiparallel to the screening field due to σ ($\sigma > 0$, $\mathcal{E} < 0$ or $\sigma < 0$, $\mathcal{E} > 0$) are all calculated with $\sigma > 0$ and $\mathcal{E} < 0$ and reversed with respect to $P_\eta = 0$ when necessary.

As discussed before, the energy curve at zero field has the appearance of a symmetric *triple-well* profile, with two metastable ferroelectric states (with 2DEG) and a central paraelectric minimum [see curve at the top in Fig. 5(a)]. As with the typical ferroelectric double-well energy landscape, the effect of the external field is to tilt the energy curves, modifying the relative stability of the different equilibrium configurations and the potential barriers. The energy curves in Fig. 5(a) demonstrate that the application of an external field can be used to switch between the paraelectric (without 2DEG) and polarized (with 2DEG) states. Most interestingly, the tristability of the energy curves in Fig. 5(a) suggests that the metal-insulator transitions should display a rather complex hysteresis. In the following lines, we use the energy curves in Fig. 5(a) to understand the shape of the hysteresis loop depicted in Fig. 5(b), obtained using the parameters that correspond to a 9-nm-thick PbTiO₃ thin film. As shown in Fig. 5(a), at zero electric field both the paraelectric ($\sigma = 0$, $P_\eta = 0$) and ferroelectric ($\sigma \sim P_\eta \sim 0.6 P_S$) configurations are stable, with the former being the ground state of the ferroelectric film [point A in panels (a) and (b) of Fig. 5]. As we increase the magnitude of the external field, the minimum of the $\sigma \neq 0$ curve deepens, eventually becoming the most stable phase of the system. However, there is a potential barrier separating the two stable phases, thus, for small fields ($\mathcal{E} \lesssim 0.2 P_S/\varepsilon_0$), starting in a configuration with $\sigma = 0$, the system can remain in the paraelectric phase (B). Nevertheless, for a high enough field the system eventually overcomes the potential barrier and the monodomain configuration as well as the 2DEG are switched on (C). If then the electric field is decreased, a potential barrier prevents the transition back to the paraelectric phase (D). The switching takes place for negative fields for which the polar configuration is no longer stable (E). For this particular thickness (9 nm), when the energy curve for $P > 0$, $\sigma \neq 0$ loses its minimum, there still exists an energy barrier separating the $\sigma = 0$ state from the one with $P < 0$ and $\sigma \neq 0$, thus, the system remains in the insulating phase (E). Therefore, for this thickness, the switching of the polarization and surface free charge polarity occurs through the nonpolar phase. Eventually, for large enough fields the system switches again to a ferroelectric state with a metallic interface (F).

Assuming the typical geometry depicted in Fig. 1(c), an ideal *interface* free of defects, and the widely accepted situation in which free charge at the *surface* gets trapped by defects or adsorbed molecules, the reversal of the polarization implies a switching between a 2DEG and a 2DHG at the buried interface. This is an interesting result, because a 2DHG has never been observed in LaAlO₃/SrTiO₃. The absence of conductivity at the *p*-type interface is commonly attributed to the fact that the polarity of the AlO₃/SrO boundary is screened by defects formed during the growth process. For the system discussed here, after the deposition the interface is buried and protected from further redox reactions. If the ferroelectric is polarized down as grown, one would expect to initially find the 2DEG, which is less susceptible to be screened by defects, at the interface, then a switching of the polarization might be able to induce the formation of the elusive 2DHG. Since
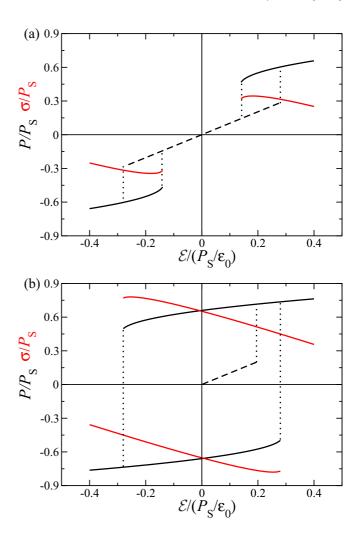

FIG. 6. (Color online) Hysteresis loop for the polarization (black line) and surface free charge (red line) as a function of the applied electric field for a ferroelectric thin film of two different thicknesses: (a) 7.5 nm ($d < d_c \sim 8.3$ nm) and (b) 10 nm (representative of the $d \gg d_c$ situation).

electrons and holes can and usually do present very different characteristics (such as mobility), this possibility constitutes an interesting opportunity for the design of new electronic devices based on oxide interfaces, where one could not only play with the on and off switching of the 2DEG, but also with the switching between different gases.

Another interesting aspect of this system is the fact that the shape of the hysteresis loop is strongly dependent on the thickness of the ferroelectric film. Figure 6(a) illustrates the case of a ferroelectric film with a thickness below the critical one for the stability of the polar configuration at zero field. In this case, the switching displays two separate loops centered at $|\mathcal{E}| > 0$. The electric field can be used to induce the transition from insulating to metallic interface, but the 2DEG would be volatile. This hysteresis loop resembles the one corresponding to an antiferroelectric, displaying a phase transition to a polar state induced by an external electric field and an absence of remnant polarization at zero field. Such features maximize the electrostatic energy that can be stored in a capacitor and suggests that hysteresis loops in ferroelectric thin films might
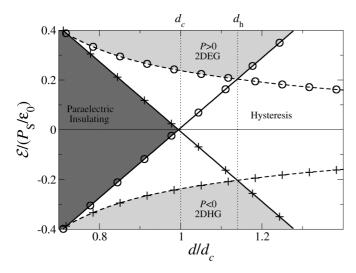
FIG. 7. Phase diagram as a function of thickness d and external electric field $\mathcal{E}$ for a PbTiO$_3$ thin film. Circles (crosses) indicate an upward (downward) jump in polarization in forward (backward) sweep. Solid (dashed) lines correspond to transitions from $\sigma \neq 0$ ($\sigma = 0$) to $\sigma = 0$ ($\sigma \neq 0$). Regions of paraelectricity and ferroelectricity (with 2DEG or 2DHG) coexistence) are shown in dark and light gray, respectively. In white, different states are accessible depending on the sweeping history.

be tailored and optimized for energy storage applications [50]. In the opposite limit of large thicknesses, shown in Fig. 6(b), once the $\sigma \neq 0$ state has been reached, the switching takes place directly between polar states, i.e., between a 2DEG and a 2DHG.

The whole phase diagram for PbTiO$_3$ thin films as a function of d and $\mathcal{E}$, including the hysteresis regions, is shown in Fig. 7. There, the regions of paraelectricity and ferroelectricity (with 2DEG or 2DHG coexistence) are shown in dark and light gray, respectively. In white, different states are possible depending on the sweeping history. For $d < d_c$, at zero field, the ferroelectric state is not stable and two separate hysteresis loops are observed at finite field, as in Fig. 6(a). In Fig. 7, d_h marks the thickness above which the switching occurs directly between the two polar states, as in Fig. 6(b). In the region between d_c and d_h, all three situations ($\sigma \neq 0$, $P > 0$), ($\sigma \neq 0$, $P < 0$), and ($\sigma = 0$) are accessible, as in Fig. 5. The phenomenology presented in Fig. 7 should be quite general, but the shapes of the different boundaries between regions of the phase diagram depend on the parameters of the material, most notably on the DOS g.

At this point, it is worth noting that the effect of a finite DOS in the model cannot be neglected to get the right dependence of polarization and free charge with the electric field. In the limit of $g \to \infty$, starting from the paraelectric phase and as the electric field increases, the system would eventually switch to the ferroelectric/2DEG state. However, once in the ferroelectric/2DEG state, if the electric field is reversed, since there is no penalty for σ to grow indefinitely (its dependence with the electric field is linear, as in the $\sigma\Delta$ term), the system would never switch back to paraelectric or to the opposite polarization state. In fact, under the $g \to \infty$ approximation, the shape of energy curve of the $\sigma \neq 0$ configurations does not change with the application of an electric field (it only shifts

up or down), therefore, the energy minimum corresponding to the ferroelectric state is a metastable configuration for any value of the electric field.

We have assumed here that the free charge can freely move from one interface or surface of the ferroelectric to the other, implying that no potential barriers are involved in these charge-transfer processes. This might be reasonable for very thin ferroelectric films (where tunneling between the two interfaces is easy) and if the potential barriers for redox reactions at the surface are relatively low. Instead, if after the formation of the 2DEG the screening charge cannot respond to an external electric field (this can be the case of free charge created after an electronic reconstruction in a relatively thick film), the polarization would be pinned by the free charge and the ferroelectric would behave as a linear dielectric with a very small susceptibility. This problem may be overcome by contacting the interface with electrodes, puncturing through the ferroelectric layer. The metallic contacts could act as the source of free charge for the modulation of the 2DEG at the interface.

IV. DISCUSSION

A. Competition with polarization domains

In the analysis presented so far we have assumed that no polarization domains are formed within the ferroelectric. This competing screening mechanism, however, constitutes the main obstacle for the formation of a 2DEG in a ferroelectric thin film. Both the electronic reconstruction or the redox processes are possible sources of screening that can help to stabilize monodomain phases in ferroelectric thin films where alternative mechanisms (such as metallic electrodes) are not present. Nevertheless, the breaking into polarization domains competes with the processes discussed here since in a fully compensated polydomain configuration the net polarization charge at surfaces or interfaces is zero, eliminating the driving force for an eventual electronic reconstruction or surface electrochemical processes.

Experiments on ferroelectric thin films grown on insulating substrates are abundant in the literature. In the following lines, we review the most relevant experimental literature in order to find potential test cases where the hypothesis presented here could be investigated. We only discuss here those experiments where the ferroelectric material is grown directly in contact with the insulator since the presence of a buffer metallic electrode would screen the polar discontinuity at the interface.

1. PbTiO$_3$/SrTiO$_3$

The most widely studied ferroelectric heterointerface is probably the case of PbTiO$_3$ thin films on SrTiO$_3$ substrates. In Refs. [17,18], for instance, authors used x-ray diffraction methods to determine the polarization distribution of PbTiO$_3$ films on SrTiO$_3$. In Ref. [17], a 10-nm film was found to be monodomain as grown with the polarization pointing down (i.e., towards the substrate). Instead, in Ref. [18] a transition with thickness was observed from polydomain (10- and 20-nm-thick films) to monodomain with the polarization pointing up (40-nm-thick films). References [19,20] investigate the phase diagram of PbTiO$_3$ thin films with respect to temperature

and thickness. Ferroelectric films with thicknesses ranging from 0.4 (1 unit cell) to 42 nm were grown on $SrTiO_3$ substrates and the polarization configuration was explored using x-ray scattering. At room temperature, polydomain phases were observed for thicknesses as small as 1.2 nm (3 unit cells). For $d \gtrsim 2$ nm, satellite peaks in the x-ray scattering maps disappear but tetragonality is consistent with polar $PbTiO_3$, suggesting a transition to a monodomain phase. Atomic force microscopy measurements were also consistent with a transition from polydomain to monodomain in thicker films [51].

Using coherent Bragg rod analysis, Fong *et al.* were able to obtain a real-space mapping of the atomic positions (and thus of the polarization) in $PbTiO_3/SrTiO_3$ interfaces [21]. The authors analyze $PbTiO_3$ films with thicknesses of 1.6 and 3.6 nm that, depending on the cooling process after growth, can be stabilized either in a monodomain (slow cooling down to room temperature) or a polydomain phase (fast cooling to 181 °C). The technique used in this work is sensitive to the local electronic density and *a priori* could be used to image the free charge accumulated to screen the polar catastrophe at the interfaces. However, this would require comparing the electronic density of a single sample in the monodomain and polydomain configurations (for which no electronic transfer is expected). Unfortunately, in the paper polydomain and monodomain phases could only be compared *in two different samples* and any difference in the surface termination and interface intermixing obscures the possible presence of screening charge.

Despite the discrepancies about the transition thickness for polydomain to monodomain phase (that might be ascribed to different growth and characterization conditions), the phase diagram that is obtained from this collection of experiments is consistent with the one provided in Refs. [20,51]. This phase diagram results from the compilation of all the experiments discussed above and shows that, at room temperature, for very small thicknesses films are paraelectric, and as the thickness is increased the ferroelectric films evolve from paraelectric to polydomain and then (in a "sluggish transition," in the words of the authors) to a monodomain phase. This suggests that films are polydomain immediately after deposition but became monodomain as they are cooled down (unless quenching is used to freeze the polydomain structure). The driving force for the transition is possibly the fact that the orientation of the polarization affects the reaction energies of the relevant redox processes at the surface, what might make one set of domains more energetically favorable than the other.

2. BaTiO₃/SrTiO₃

In Ref. [22], authors study $BaTiO_3$ films grown on $SrTiO_3$ substrates. $SrTiO_3$ exerts a compressive strain on $BaTiO_3$ stabilizing a tetragonal phase. In this work, a combination of UV Raman spectroscopy and synchrotron x-ray scattering is used to test the polarity of films with thicknesses of 1.6 to 10 nm. It is found that films of all thicknesses are polar at low temperature. At room temperature, films capped with a 10-nm $SrTiO_3$ layer were polydomain with regular domain sizes. X-ray scattering spectra of uncapped films did not show satellite peaks, but authors were not able to establish whether

this was due to nonperiodic domains, domain sizes larger than the experimental resolution, or stabilization of a monodomain phase. The model proposed here might offer a possible interpretation of this experiment. The uncapped samples could sustain a monodomain phase screened by the accumulation of free charge at the interface and surface. In the capped films, there would be two possible ways for stabilizing a monodomain configuration. (i) Redox processes at the $SrTiO_3$ surface could provide the necessary free charge to screen the polar discontinuity at the ferroelectric/substrate interface, but then the capping $SrTiO_3$ layer should be polarized as well, with the corresponding energy cost. (ii) Electronic reconstruction within the ferroelectric layer could simultaneously screen the polar discontinuity at both interfaces (with the electrode and the capping layer), but the value of Δ for this process is much larger than for the surface electrochemical reactions. In either case, the energy cost of a monodomain polarization in the capped film would be higher than for the uncapped one, consistent with the observation of polydomain phases in the capped samples.

In Ref. [23], authors report ferroelectricity in $BaTiO_3/SrTiO_3/SiO_2/Si$ heterostructures. Even without a top electrode, authors claim that polarization can be written in $BaTiO_3$ films as thin as 8 nm with the tip of an atomic force microscope. For thicknesses of 1.6 nm or below, written domains were unstable. They also report hysteresis loops in the piezoelectric response without top electrode.

All these experiments, and especially the phase diagram for $PbTiO_3$ films on $SrTiO_3$ substrates provided in Ref. [51], consistently support the possibility of stabilizing a monodomain phase in ferroelectric thin films grown directly on insulating substrates. Unfortunately, the source of screening required to stabilize such configuration is discussed in very little detail and the possibility of an electronic reconstruction or alternative process that could form a 2DEG or 2DHG at the interface was not contemplated in those works. Very recently, however, the formation of a 2DEG at the interface between $CaZrO_3$ and $SrTiO_3$ has been reported [52]. Even if $CaZrO_3$ is not polar in bulk, it is argued in Ref. [52] that the compressive strain exerted by the substrate might induce a polarization of the $CaZrO_3$ which would be responsible for the formation of the 2DEG. Although ferroelectricity (switchable polarization) could not be demonstrated, the evolution of the free charge with thickness is in good agreement with the model presented here. Further characterization of electromechanical and transport properties in samples similar to those discussed in this section, and the comparison with the results of the model would be critical to assess the hypothesis presented here.

3. A model for the competition with polarization domains

The model discussed in Sec. II takes into account the balance of the monodomain ferroelectricity with a paraelectric phase, but cannot say anything about the competition with a polydomain phase. Since experiments demonstrate that such a competition exists and the balance is delicate, here we use a simple model to investigate the relative stability of these two phases.

Since the two screening mechanisms are mutually exclusive we do not need to add new terms to our energy expression of

Eq. (8). Instead, to analyze the competition between the two phases (monodomain and polydomain), we need to compare the thickness evolution of the energy of a thin film in the two different scenarios. For the polydomain phase, we assume a 180° domain structure, in which straight stripes of the material, all with the same width in the direction perpendicular to the domain wall, have an out-of-plane polarization of the same magnitude but with alternating orientations. For such idealized version of the domain structures typically found in tetragonal ferroelectric thin films, the energy per unit of volume of the polydomain phase can be expressed as

$$G_{\text{poly}} = U + \frac{\Sigma}{w} + G_{\text{elec}}, \quad (26)$$

where Σ is the energy per unit of area of a domain wall and w is the domain width. The electrostatic energy G_{elec} due to stray fields in the polydomain configuration is proportional to the domain width [53,54] $G_{\text{elec}} = \gamma w/d$, where the proportionality constant can be calculated to be

$$\gamma = \frac{8.416 P^2}{\pi^3 \varepsilon_0 [1 + (\varepsilon_x \varepsilon_z)^{1/2}]} \quad (27)$$

for 180° stripe domains [55]. The width of domain walls in a typical ferroelectric is vanishingly small and remnant electric fields in polydomain configurations decay exponentially away from the surface and the domain wall, thus, except in the limit of thicknesses of a few unit cells, we can approximate $|P| \sim P_S$ throughout the film and $U = U_0(P_S)$ as a constant. Using this result and differentiating Eq. (26) with respect to w to find the equilibrium domain width for a given thickness of the film, one obtains the well-known Kittel law [53]

$$w^2 = \frac{\Sigma d}{\gamma}. \quad (28)$$

Substituting this expression for the equilibrium domain width into Eq. (26) leads to the following expression for the energy per unit volume:

$$G_{\text{poly}}(d) = U_0(P_S) + 2\left(\frac{\Sigma \gamma}{d}\right)^{1/2}. \quad (29)$$

In Eq. (29), the first term is negative and constant, independent of the thickness of the film; the second one is positive, diverges at $d \to 0$ (due to the divergence of the domain-wall density given by the Kittel law), and decays with the thickness of the ferroelectric.

The Kittel law has been shown to be valid down to thicknesses of a few nanometers in typical ferroelectric thin films [56,57]. This simplified expression for the energy is expected to break down below the limit of a few unit cells, at which point one should take into account the finite width of the domain wall, the stray fields, and the inhomogeneities of the polarization inside the domains. Neglecting these effects, and using again the parameters obtained from first-principles simulations for PbTiO₃ [30], we compare the energy of the polydomain configuration of Eq. (29) (red curve in Fig. 8) with that of a monodomain phase where we allow the possibility of having surface charge, as discussed in Sec. II A, given by Eq. (8) (black curve in Fig. 8). As demonstrated before, ferroelectricity in a monodomain phase becomes stable only above a critical thickness $d > d_c$. In Fig. 8, we are plotting the
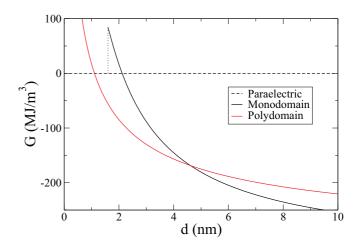

FIG. 8. (Color online) Energy density of a ferroelectric thin film in monodomain (black curve) and polydomain (red curve) states. Curves are calculated for bulk PbTiO₃, in the limit of $g \to \infty$, using parameters obtained from first-principles calculations [30]. In this plot $\Delta = 1$ V, realistic for surface redox processes.

case where $\Delta = C/Q \sim 1$ V, corresponding to a screening by surface redox processes, that yields a value of $d_c = 1.60$ nm. Interestingly, even though for small thicknesses the model predicts that the most favorable scenario is the formation of polarization domains, it also shows that there should be a crossover between the two phases, such that above a critical thickness the stabilization of a monodomain state by the formation of a 2DEG would become energetically favorable over the breaking into domains of polarization. For the chosen parameters, this crossover takes place for a thickness of about 4.6 nm, well within the range of thicknesses that are typically grown in ferroelectric thin-film experiments. The thickness at which the transition from a polydomain to a monodomain configuration takes place strongly depends on the value of Δ. This parameter takes different values depending on the screening mechanism we are considering: it is simply the band gap of the ferroelectric if we are assuming an electronic reconstruction scenario in a free-standing slab, and $\Delta = C/Q$ if we consider the possibility of having electrochemical processes taking place at the free surfaces of the material. In the first case, it is obvious that the band-gap underestimation by the traditional exchange-correlation functionals would greatly affect the estimated crossover thickness obtained from DFT calculations, as shown in Table III. In the case of a ferroelectric thin film on top of a substrate, the relevant gap Δ would depend also on the band gap of the substrate material and the band alignment at the interface, as indicated in Fig. 1.

TABLE III. Estimated thickness for the monodomain to polydomain crossover d_{c-o} in PbTiO₃ thin films. Parameters for the model have been obtained from first-principles simulations [30].

	Δ (V)	d_{c-o} (nm)
Redox processes	$C/Q \sim 1$	4.6
LDA gap	1.45	10
Expt. gap	3.6	64

TABLE IV. Estimated thickness for the monodomain to polydomain crossover in thin films of $BiFeO_3$ under a compressive strain of 5%. The parameters for the model have been obtained from first-principles simulations available in the literature (see text) except for the relative permittivity, that was calculated here ($\varepsilon_x = 35$, $\varepsilon_z = 25$). Formation of a 2DEG by means of surface redox processes is more favorable than polydomain configurations for all thicknesses.

	Δ (V)	d_{c-o} (nm)
Redox processes	$C/Q \sim 1$	0
Expt. gap	3.1	8.7

PbTiO$_3$ was chosen as an example to test the model presented here because it is a prototypical ferroelectric and has good characteristics to exhibit the formation of the 2DEG at reasonable thicknesses, as demonstrated by the values in Tables I and III. But in fact one could now use Eqs. (29) and (8) to explore scenarios that could favor even further the formation of a 2DEG over the domains of polarization. Ideally, one would like to find a material with large domain-wall energy and spontaneous polarization and small band gap and dielectric constant. A good candidate could be the so-called "super tetragonal" phase of BiFeO$_3$ (at least from a theoretical point of view, experimentally the stabilization of these phases requires a large in-plane compressive strain and the material usually forms a mixed phase with other monoclinic phases of BiFeO$_3$ [58]; another disadvantage of this material is that experimental samples often present a very large leakage, behaving like a semiconductor more than like a true insulator). First-principles simulations predict that for in-plane compressive strains larger than $\sim$5% some phases of BiFeO$_3$ could display a spontaneous polarization [59,60] of up to 150 C/m^2 and domain-wall energies [61] of about 250 mJ/m^2. A band gap of 3.1 eV has been obtained by optical absorption measurements in these highly strained phases [62]. All these parameters would yield an estimated crossover thickness for the transition from polydomain to monodomain of 8.7 nm in the electronic reconstruction scenario. Furthermore, if the monodomain polarization is stabilized by surface electrochemical reactions, this phase is more favorable than the polydomain for any thickness, as shown in Table IV.

This result suggests that even if the breaking up into domains is a very effective mechanism for the screening of the polar discontinuity at the surface or interface in a ferroelectric thin film, the formation of a 2DEG is indeed viable and might form for an appropriate combination of materials and boundary conditions. The prediction, using such a simple model, of a transition from polydomain to monodomain as the thickness is increased is in good agreement with the experimental observations and should constitute a further motivation to explore the scenario proposed here.
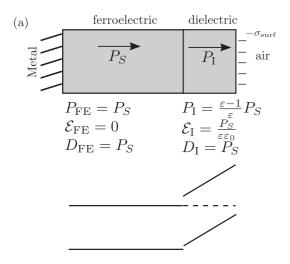
B. Ferroelectric substrate

If the ferroelectric material is the substrate, and the film is a dielectric perovskite, the situation is different. If the substrate is thick and is connected to a metal at the back, the polarization discontinuity at the ferroelectric/metal interface would be screened and the ferroelectric would display a strong tendency to develop a finite polarization. This, however, gives rise to a polarization mismatch at the ferroelectric/dielectric overlayer interface that needs to be compensated to fully screen the depolarizing field. In fact, the problem shares many similarities with the LaAlO$_3$/SrTiO$_3$. In the latter case, the thick substrate imposes $D = 0$ electrostatic boundary conditions. Since LaAlO$_3$ has a finite polarization at zero electric field, the $D = 0$ condition implies that an electric field develops inside the polar material. For a thin LaAlO$_3$ film, the material polarizes under the action of the field, tending to reduce the polar discontinuity. Above a critical thickness, though, an electronic reconstruction (or a more complex mechanism possibly involving redox processes) becomes more energetically favorable and a 2DEG forms at the interface. Instead, in the case of a nonpolar dielectric layer on top of a thick ferroelectric substrate, the thick ferroelectric imposes $D = P_S$. As in the case of the LaAlO$_3$, in the absence of free charge at the interface this condition induces an electric field in the insulating top layer, which for small thicknesses will polarize [see Fig. 9(a)] until, as the thickness increases, the energy balance favors formation of a 2DEG at the interface [see Fig. 9(b)]. There are two important differences with respect to the LaAlO$_3$/SrTiO$_3$ case though. In the case of the ferroelectric substrate/dielectric film a polar discontinuity exists also at the free surface of the dielectric film, which requires the accumulation of some superficial free charge (most likely provided by chemical adsorbates, schematically represented by negative signs in Fig. 9, in accordance with the choice of polarization orientation in the ferroelectric) even before the screening at the interface sets in. But, most importantly, in this system ΔP can be changed (switched) by an electric field and by temperature.

Consider, for example, an SrTiO$_3$ film on a BaTiO$_3$ substrate. In this case, ΔP is the bulk polarization of the substrate (at low T analogous in magnitude to the polarization mismatch in LaAlO$_3$/SrTiO$_3$), and there would be then an instability with a similar critical thickness of the film for either electronic reconstruction, the appearance of redox defects, or both. Assuming that beyond that critical thickness equilibrium is established in the presence of a bulk polarization of BaTiO$_3$ parallel to z, a 2DEG should appear at the interface, of electrons for one sign of BaTiO$_3$'s polarization, of holes for the other. If switching the substrate ferroelectric, and assuming equilibrium, the gas of electrons should transform into gas of holes and vice versa. Alternatively, one could think of a 2DEG (or 2DHG) being switched on and off with T if, say, starting from BaTiO$_3$ above the ferroelectric critical T, and letting it cool down until it polarizes enough to give rise to the gas.

Finally, if one is interested in switching on and off the 2DEG with a transversal electric field, a polar film can be considered, such as LaAlO$_3$, and a ferroelectric substrate chosen such that its bulk polarization at the temperature of operation is close to the LaAlO$_3$ half-quantum. With both polarizations aligned, $\Delta P \sim 0$ and no 2DEG should arise. If the ferroelectric is then switched, ΔP becomes approximately a whole quantum, and the 2DEG should be strongly populated and stable for quite a thin film, possibly allowing for the Zener tunneling to take place populating the 2DEG. In this geometry, for either configuration there would still be a polarization discontinuity at the free surface, but this would probably be screened by redox processes.

(a)   ferroelectric   dielectric

$$P_{\mathrm{FE}} = P_S \qquad\qquad P_{\mathrm{I}} = \frac{\varepsilon - 1}{\varepsilon} P_S$$
$$\mathcal{E}_{\mathrm{FE}} = 0 \qquad\qquad\quad \mathcal{E}_{\mathrm{I}} = \frac{P_S}{\varepsilon \varepsilon_0}$$
$$D_{\mathrm{FE}} = P_S \qquad\qquad D_{\mathrm{I}} = P_S$$

(b)   ferroelectric   dielectric

$$P_{\mathrm{FE}} = P_S \qquad\qquad P_{\mathrm{I}} = \frac{\varepsilon - 1}{\varepsilon} (P_S - \sigma)$$
$$\mathcal{E}_{\mathrm{FE}} = 0 \qquad\qquad\quad \mathcal{E}_{\mathrm{I}} = \frac{P_S - \sigma}{\varepsilon \varepsilon_0}$$
$$D_{\mathrm{FE}} = P_S \qquad\qquad D_{\mathrm{I}} = P_S - \sigma$$
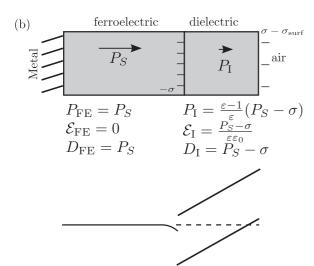
FIG. 9. Schematic depiction of the electrostatics involved in the case of an insulating thin film on top of a ferroelectric substrate, both (a) before and (b) after an electronic reconstruction. A schematic band diagram of the system is shown at the bottom of each panel. Note that for this geometry, even before the electronic reconstruction, free charges need to be present at the surface to screen the polar discontinuity with the vacuum/air region.

C. Hyperferroelectrics

Recently, a new family of ferroelectric materials has been discovered that are predicted to display a finite polarization at $D = \sigma = 0$, hence, the reason why they were named *hyperferroelectrics* [25]. Their capacity to display a finite polarization even in the absence of any source of screening might give the impression that the tendency of these materials to display 2DEG is even stronger than for traditional ferroelectrics. For this reason, in this section we present an analysis for these materials similar to the one carried out in Sec. II A. Hyperferroelectrics are fundamentally equivalent to conventional ferroelectrics in the sense that the ferroelectric phase transition is driven by an unstable polar mode. Even though their behavior in open circuit boundary conditions is radically different from that of conventional ferroelectrics, the underlying physics is completely analogous. The fundamental

differences are the low effective charges associated with the polar mode and the large polarizability of the electronic cloud. The consequence of this is that in open boundary conditions the electronic polarization screens the zero-field contribution and a large fraction of the polar distortion remains stable. As demonstrated in Ref. [25], these materials are expected to display a small but finite remnant polarization at $D = 0$.

Since the basic mechanism for ferroelectricity in hyperferroelectrics is the same as for traditional ferroelectrics, the expression of the free energy for these materials is again Eq. (8). One can, in fact, use that expression to find the condition for a ferroelectric to behave as a hyperferroelectric by calculating the equilibrium polarization for $\sigma = 0$. Using Eq. (19) with $\sigma = 0$ and differentiating with respect to the polarization, one obtains the equilibrium condition

$$\frac{P_\eta^3}{P_S^3} + \frac{P_\eta}{P_S} \left(\frac{2\chi_\eta}{\varepsilon_\infty} - 1 \right) = 0. \tag{30}$$

This equation has solutions

$$P_\eta^{D=0} = 0; \qquad P_\eta^{D=0} = \pm \sqrt{1 - \frac{2\chi_\eta}{\varepsilon_\infty}}. \tag{31}$$

The nonzero solutions are real only if $\varepsilon_\infty > 2\chi_\eta$, which constitutes the condition for hyperferroelectricity.

Here, we perform an analysis completely analogous to the one in Sec. II A to obtain the evolution of polarization and free charge in a thin film of a hyperferroelectric. We use the set of parameters corresponding to LiBeSb reported in Ref. [25] ($\chi_\eta \sim 6$ is estimated from the curvature at the minimum of the double-well potential). The result is plotted in Fig. 10. Three important differences are observed in the curves of Fig. 10 with respect to the corresponding ones for a traditional ferroelectric in Fig. 2. First, as expected for these materials, for a thickness below the onset for the electronic reconstruction the material displays a large polar distortion that is effectively screened by the electrons, resulting in a small but finite total
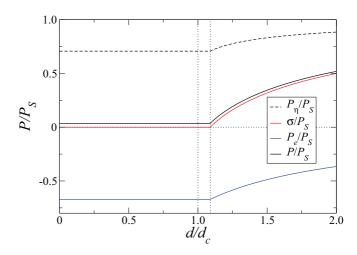

FIG. 10. (Color online) Total polarization (black solid line), zero-field contribution (dashed line), electronic contribution (solid blue line), and surface free charge (solid red line) as a function of thickness. d_c is the one given by Eq. (13) and in this case it does not mark the critical thickness for 2DEG formation.

polarization at $D = \sigma = 0$. Second, the 2DEG becomes stable at a thickness larger than the critical one given by Eq. (13). Finally, neither the total polarization nor the free charge display a discontinuous jump at the transition. In fact, the second and third observations are connected. Using Eqs. (10), (13), and (14), one can demonstrate that the value of the free charge at d_c is

$$\sigma_c = \frac{P_S}{\sqrt{3}}\left(1 - \frac{\varepsilon_\infty}{3\chi_\eta}\right). \tag{32}$$

This expression yields negative values of σ for $\varepsilon_\infty > 3\chi_\eta$, which are not a valid solution of the model. Therefore, for those materials with $\varepsilon_\infty > 3\chi_\eta$, like LiBeSb, σ goes to zero (the 2DEG vanishes) in a continuous transition and for a thickness larger than d_c. The range of $2\chi_\eta < \varepsilon_\infty < 3\chi_\eta$ constitutes a third regime in the phase diagram with respect to $\varepsilon_\infty/\chi_\eta$, where the material is a hyperferroelectric but still displays a discontinuous jump in the polarization and the free charge.

As demonstrated in Ref. [25], the small but finite polarization at $D = \sigma = 0$ is a consequence of the strong screening provided by the large electronic polarizability, but the ferroelectric instability is not necessarily stronger than in normal ferroelectrics. We have seen in this section that the use of hyperferroelectrics does not favor the formation of a 2DEG as compared with a traditional ferroelectric, and in fact some of the most remarkable features of this system might be lost, such as the discontinuous transition of the polarization.

V. CONCLUSIONS

We have used a simple model to demonstrate that under the appropriate conditions, a monodomain out-of-plane polarization may be stabilized in a ferroelectric thin film grown directly on an insulating substrate through the formation of a 2DEG at its interface. Although there are important analogies with the related polar interfaces between dielectric materials, of which $LaAlO_3/SrTiO_3$ is the prototypical example, there are striking differences in behavior too. For the 2DEG at ferroelectric interfaces, the model predicts that a discontinuous transition as a function of thickness takes place between the paraelectric (without 2DEG) and the ferroelectric (with 2DEG) phases, with an abrupt jump in both polarization and free charge. Also, in contrast with the $LaAlO_3/SrTiO_3$, we have demonstrated that the thickness for this transition strongly depends on the DOS of the 2DEG.

One of the key features that was sought in this system was the ability to switch on and off the 2DEG as well as between a 2DEG and a 2DHG with the application of an external electric field. The model shows a complex hysteresis behavior, an effect that poses interesting possibilities for energy storage and nonvolatile memory applications.

The model has also been used to discuss possible strategies to favor this state over the competing paraelectric and poly-domain configurations. We hope that the predictions derived from the model, supported by the first-principles simulations and some of which agree with many features from available experiments, will motivate the search for 2DEG in these systems.

ACKNOWLEDGMENTS

[1] A. Ohtomo, D. A. Muller, J. L. Grazul, and H. Y. Hwang, Nature (London) **419**, 378 (2002).

[2] A. Ohtomo and H. Y. Hwang, Nature London) **427**, 423 (2004).

[3] N. Reyren, S. Thiel, A. D. Caviglia, L. F. Kourkoutis, G. Hammerl, C. Richter, C. W. Schneider, T. Kopp, A.-S. Rüetschi, D. Jaccard, M. Gabay, D. A. Muller, J.-M. Triscone, and J. Mannhart, Science **317**, 1196 (2007).

[4] L. Li, C. Richter, S. Paetel, T. Kopp, J. Mannhart, and R. C. Ashoori, Science **332**, 825 (2011)

[5] M. Stengel and D. Vanderbilt, Phys. Rev. B **80**, 241103(R) (2009).

[6] N. Nakagawa, H. Y. Hwang, and D. A. Muller, Nat. Mater. **5**, 204 (2006).

[7] A. Annadi, Q. Zhang, X. Renshaw Wang, N. Tuzla, K. Gopinadhan, W. M. Lü, A. Roy Barman, Z. Q. Liu, A. Srivastava, S. Saha, Y. L. Zhao, S. W. Zeng, S. Dhar, E. Olsson, B. Gu, S. Yunoki, S. Maekawa, H. Hilgenkamp, T. Venkatesan, and Ariando, Nat. Commun. **4**, 1838 (2013).

[8] M. L. Reinle-Schmitt, C. Cancellieri, D. Li, D. Fontaine, M. Medarde, E. Pomjakushina, C. W. Schneider, S. Gariglio, P. Ghosez, J.-M. Triscone, and P. R. Willmott, Nat. Commun. **3**, 932 (2012).

[9] S. Thiel, G. Hammerl, A. Schmehl, C. W. Schneider, and J. Mannhart, Science **313**, 1942 (2006).

[10] N. C. Bristowe, E. Artacho, and P. B. Littlewood, Phys. Rev. B **80**, 045425 (2009).

[11] C. W. Bark, D. a. Felker, Y. Wang, Y. Zhang, H. W. Jang, C. M. Folkman, J. W. Park, S. H. Baek, H. Zhou, D. D. Fong, X. Q. Pan, E. Y. Tsymbal, M. S. Rzchowski, and C. B. Eom, Proc. Natl. Acad. Sci. USA **108**, 4720 (2011).

[12] V. T. Tra, J.-W. Chen, P.-C. Huang, B.-C. Huang, Y. Cao, C.-H. Yeh, H.-J. Liu, E. a. Eliseev, A. N. Morozovska, J.-Y. Lin, Y.-C. Chen, M.-W. Chu, P.-W. Chiu, Y.-P. Chiu, L.-Q. Chen, C.-L. Wu, and Y.-H. Chu, Adv. Mater. **25**, 3357 (2013).

[13] M. K. Niranjan, Y. Wang, S. S. Jaswal, and E. Y. Tsymbal, Phys. Rev. Lett. **103**, 016804 (2009).

[14] Y. Wang, M. K. Niranjan, S. S. Jaswal, and E. Y. Tsymbal, Phys. Rev. B **80**, 165130 (2009).

[15] K. D. Fredrickson and A. A. Demkov, Phys. Rev. B **91**, 115126 (2015).

[16] P. García-Fernández, P. Aguado-Puente, and J. Junquera, Phys. Rev. B **87**, 085305 (2013).

[17] C. Thompson, C. M. Foster, J. A. Eastman, and G. B. Stephenson, Appl. Phys. Lett. **71**, 3516 (1997).

[18] M. J. Bedzyk, A. Kazimirov, D. L. Marasco, T.-L. Lee, C. M. Foster, G.-R. Bai, P. F. Lyman, and D. T. Keane, Phys. Rev. B **61**, R7873 (2000).

[19] S. K. Streiffer, J. A. Eastman, D. D. Fong, C. Thompson, A. Munkholm, M. V. Ramana Murty, O. Auciello, G. R. Bai, and G. B. Stephenson, Phys. Rev. Lett. **89**, 067601 (2002).

[20] D. D. Fong, G. B. Stephenson, S. K. Streiffer, J. A. Eastman, O. Auciello, P. H. Fuoss, and C. Thompson, Science **304**, 1650 (2004).

[21] D. D. Fong, C. Cionca, Y. Yacoby, G. B. Stephenson, J. A. Eastman, P. H. Fuoss, S. K. Streiffer, C. Thompson, R. Clarke, R. Pindak, and E. A. Stern, Phys. Rev. B **71**, 144112 (2005).

[22] D. A. Tenne, P. Turner, J. D. Schmidt, M. Biegalski, Y. L. Li, L. Q. Chen, A. Soukiassian, S. Trolier-McKinstry, D. G. Schlom, X. X. Xi, D. D. Fong, P. H. Fuoss, J. A. Eastman, G. B. Stephenson, C. Thompson, and S. K. Streiffer, Phys. Rev. Lett. **103**, 177601 (2009).

[23] C. Dubourdieu, J. Bruley, T. M. Arruda, A. Posadas, J. Jordan-Sweet, M. M. Frank, E. Cartier, D. J. Frank, S. V. Kalinin, A. A. Demkov, and V. Narayanan, Nat. Nanotechnol. **8**, 748 (2013).

[24] N. C. Bristowe, P. Ghosez, P. B. Littlewood, and E. Artacho, J. Phys.: Condens. Matter **26**, 143201 (2014).

[25] K. F. Garrity, K. M. Rabe, and D. Vanderbilt, Phys. Rev. Lett. **112**, 127601 (2014).

[26] N. C. Bristowe, P. B. Littlewood, and E. Artacho, Phys. Rev. B **83**, 205405 (2011).

[27] N. A. Pertsev, A. G. Zembilgotov, and A. K. Tagantsev, Phys. Rev. Lett. **80**, 1988 (1998).

[28] A. K. Tagantsev, Ferroelectrics **69**, 321 (1986).

[29] M. Stengel, C. J. Fennie, and P. Ghosez, Phys. Rev. B **86**, 094112 (2012).

[30] We are using parameters corresponding to $PbTiO_3$ strained in plane to an implicit $SrTiO_3$ substrate. The corresponding parameters, obtained from first-principles calculations are $P_S = 0.78$ C/m^2, $\chi_\eta = 26$, $\varepsilon_\infty = 7$, $g_e/e^2 = 1.2 \times 10^{37}$ m^{-2}J^{-1}, and $g_h/e^2 = 2.5 \times 10^{37}$ m^{-2}J^{-1}. For the study of the competition with a polydomain phase we use $\Sigma = 130$ mJ/m^2 (from Ref. [63]), $\varepsilon_z = \varepsilon_\infty + (\chi_\eta + 1) = 35$, and $\varepsilon_x = 185$.

[31] A. D. Caviglia, S. Gariglio, N. Reyren, D. Jaccard, T. Schneider, M. Gabay, S. Thiel, G. Hammerl, J. Mannhart, and J.-M. Triscone, Nature (London) **456**, 624 (2008).

[32] B. Förg, C. Richter, and J. Mannhart, Appl. Phys. Lett. **100**, 053506 (2012).

[33] Z. S. Popović, S. Satpathy, and R. M. Martin, Phys. Rev. Lett. **101**, 256801 (2008).

[34] P. Delugas, A. Filippetti, V. Fiorentini, D. I. Bilc, D. Fontaine, and P. Ghosez, Phys. Rev. Lett. **106**, 166807 (2011).

[35] B. Yin, P. Aguado-Puente, S. Qu, and E. Artacho, arXiv:1506.04865.

[36] D. G. Schlom, L.-Q. Chen, C.-B. Eom, K. M. Rabe, S. K. Streiffer, and J.-M. Triscone, Annu. Rev. Mater. Res. **37**, 589 (2007).

[37] D. D. Fong, A. M. Kolpak, J. A. Eastman, S. K. Streiffer, P. H. Fuoss, G. B. Stephenson, C. Thompson, D. M. Kim, K. J. Choi, C. B. Eom, I. Grinberg, and A. M. Rappe, Phys. Rev. Lett. **96**, 127601 (2006).

[38] J. E. Spanier, A. M. Kolpak, J. J. Urban, I. Grinberg, L. Ouyang, W. S. Yun, A. M. Rappe, and H. Park, Nano Lett. **6**, 735 (2006).

[39] R. V. Wang, D. D. Fong, F. Jiang, M. J. Highland, P. H. Fuoss, C. Thompson, A. M. Kolpak, J. A. Eastman, S. K. Streiffer, A. M. Rappe, and G. B. Stephenson, Phys. Rev. Lett. **102**, 047601 (2009).

[40] G. B. Stephenson and M. J. Highland, Phys. Rev. B **84**, 064107 (2011).

[41] N. C. Bristowe, M. Stengel, P. B. Littlewood, J. M. Pruneda, and E. Artacho, Phys. Rev. B **85**, 024106 (2012).

[42] C. Cen, S. Thiel, G. Hammerl, C. W. Schneider, K. E. Andersen, C. S. Hellberg, J. Mannhart, and J. Levy, Nat. Mater. **7**, 298 (2008).

[43] Y. Li, S. N. Phattalung, S. Limpijumnong, J. Kim, and J. Yu, Phys. Rev. B **84**, 245307 (2011).

[44] L. Yu and A. Zunger, Nat. Commun. **5**, 5118 (2014).

[45] M. Stengel, N. A. Spaldin, and D. Vanderbilt, Nat. Phys. **5**, 304 (2009).

[46] J. M. Soler, E. Artacho, J. D. Gale, A. García, J. Junquera, P. Ordejón, and D. Sánchez-Portal, J. Phys.: Condens. Matter **14**, 2745 (2002).

[47] H. Monkhorst and J. Pack, Phys. Rev. B **13**, 5188 (1976).

[48] J. Moreno and J. M. Soler, Phys. Rev. B **45**, 13891 (1992).

[49] M. Hosoda, Y. Hikita, H. Y. Hwang, and C. Bell, Appl. Phys. Lett. **103**, 103507 (2013).

[50] N. Ortega, a. Kumar, J. F. Scott, D. B. Chrisey, M. Tomazawa, S. Kumari, D. G. B. Diestra, and R. S. Katiyar, J. Phys.: Condens. Matter **24**, 445901 (2012).

[51] C. Thompson, D. D. Fong, R. V. Wang, F. Jiang, S. K. Streiffer, K. Latifi, J. a. Eastman, P. H. Fuoss, and G. B. Stephenson, Appl. Phys. Lett. **93**, 182901 (2008).

[52] Y. Chen, F. Trier, T. Kasama, D. V. Christensen, N. Bovet, Z. I. Balogh, H. Li, K. T. S. Thydén, W. Zhang, S. Yazdi, P. Norby, N. Pryds, and S. r. Linderoth, Nano Lett. **15**, 1849 (2015).

[53] C. Kittel, Phys. Rev. **70**, 965 (1946).

[54] T. Mitsui and J. Furuichi, Phys. Rev. **90**, 193 (1953).

[55] T. Ozaki and J. Ohgami, J. Phys.: Condens. Matter **7**, 1711 (1995).

[56] G. Catalán, J. F. Scott, A. Schilling, and J. M. Gregg, J. Phys.: Condens. Matter **19**, 022201 (2007).

[57] G. Catalán, H. Béa, S. Fusil, M. Bibes, P. Paruch, A. Barthélémy, and J. F. Scott, Phys. Rev. Lett. **100**, 027602 (2008).

[58] R. J. Zeches, M. D. Rossell, J. X. Zhang, A. J. Hatt, Q. He, C.-H. Yang, A. Kumar, C. H. Wang, A. Melville, C. Adamo, G. Sheng, Y.-H. Chu, J. F. Ihlefeld, R. Erni, C. Ederer, V. Gopalan, L. Q. Chen, D. G. Schlom, N. A. Spaldin, L. W. Martin, and R. Ramesh, Science **326**, 977 (2009).

[59] A. J. Hatt, N. A. Spaldin, and C. Ederer, Phys. Rev. B **81**, 054109 (2010).

[60] O. Diéguez, O. E. González-Vázquez, J. C. Wojdel, and J. Íñiguez, Phys. Rev. B **83**, 094105 (2011).

[61] W. Ren, Y. Yang, O. Diéguez, J. Íñiguez, N. Choudhury, and L. Bellaiche, Phys. Rev. Lett. **110**, 187601 (2013).

[62] P. Chen, N. J. Podraza, X. S. Xu, A. Melville, E. Vlahos, V. Gopalan, R. Ramesh, D. G. Schlom, and J. L. Musfeldt, Appl. Phys. Lett. **96**, 131907 (2010).

[63] B. Meyer and D. Vanderbilt, Phys. Rev. B **65**, 104111 (2002).